Jurnal Teknologi

Full Paper

FINANCIAL-BASED ASSESSMENT IN PRACTICAL EPDS USING REACTIVE POWER SUPPORT CONSIDERING DIFFERENT LOAD VARIATIONS

R. Senthil Kumar[a], Srinivasan G.[b*], Rajan V. R.[c], Lavanya M.[d]

[a]Department of Electrical and Electronics Engineering, SRM Institute of Science and Technology, SRM University, Kattankulathur, Chengalpattu (Dt.)–603203, India
[b]Department of Electrical and Electronics Engineering, EXCEL Engineering College, Pallakkapalayam, Komarapalayam–637303, Namakkal (Dt.), Tamilnadu, India
[c]Department of Electronics and Communication Engineering, T. John Institute of Technology, Gottigere, Bannerghatta Road, Bangalore–560083, India
[d]Department of Mechatronics Engineering, Sona College of Technology, Salem–636005, Tamil Nadu, India

Article history
Received
7 February 2024
Received in revised form
11 February 2025
Accepted
12 February 2025
Published Online
24 October 2025

*Corresponding author
gsrinivasan.eec@excellcolleges.com

Graphical abstract

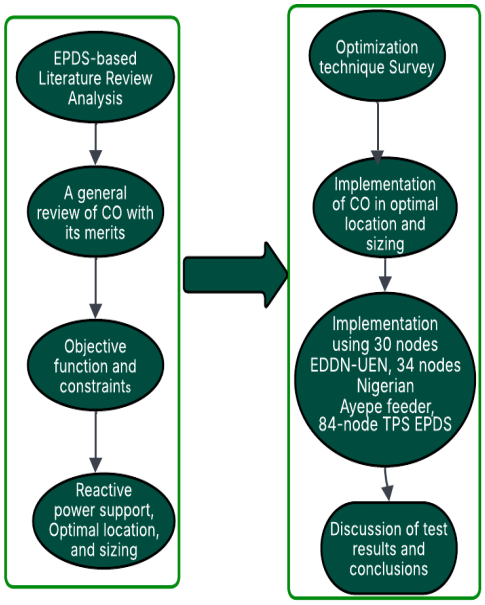

Abstract

It has been substantiated that Reactive Power Injections (RPI) at optimal locations reduce power losses (P_{LS} & Q_{LS}) and enrichment in node voltage profile, thereby enhancing efficacy. Most researchers considered the reduction in real power loss (P_{LS}) and capacitor purchase costs as objectives to get Financial Savings (FS). However, this work focuses on maximizing FS by optimal allocation and capacity determination of capacitors in Electric Power Distribution Systems (EPDS), considering the reduction in power losses and capacitor purchase and its associated costs as objective subject to satisfaction of equality and inequality constraints. Cheetah Optimizer (CO) has been considered to solve the Financial Based Objective Function (FBOF) to obtain an improved solution in this work. Researchers normally adopt a Sensitivity Based Index (SBI) to identify potential node RPIs by ranking. Nevertheless, the CO technique will do both optimal placement and sizing of capacitors. The efficacy of the projected CO has been validated using three real EPDS. The outcomes of CO have been compared with other optimization techniques available in the literature. Simulated results reveal that CO effectively minimizes power losses with considerable improvement in FS compared to other techniques.

Keywords: Cheetah optimizer, Financial savings, Electric power distribution system, Power losses, Reactive power injection

1.0 INTRODUCTION

The main challenges of modern Electric Power Distribution Systems (EPDS) are keeping the power losses at a bare minimum, and all the node voltages must be within the permissible limits. Though the Power Losses (P_{LS} & Q_{LS}) affect the entire power system, the EPDS accounts for most of it because of its high R/X ratio and radiality by nature. The increase in power losses and poor voltage profiles are due to a sharp increase in power demand over time. Several studies have reported that I^2R loss at EPDS accounts for roughly 13% of the overall energy output. [1]. Similarly, to reduce T&D losses in India, the electric power sector reforms were implemented after the year 2000, due to which the total P_{LS} dropped from 37% to 24.6% in 2001-02 [2]. Improvement in EPDS performance necessitates appropriate planning to increase the utility efficiency (i.e.) how effectively the P_{LS} gets minimized is the responsibility of the distribution utilities, thereby reducing financial loss.

Integration of capacitors with proper sizing at optimal locations will result in improved voltage regulation, reduced power/energy loss, increased feeder capacity release, improved sub-station power factor, drop in kVA demand, improved power quality, decreased payment for the energy, etc. Due to the integration of capacitors, reactive power demand on the main primary source gets reduced. Thus, more real power output is possible [3]. The optimal capacitor allocation problem has been analyzed since 1960s by many researchers. Classical, mathematical, numerical, and heuristic methods are some of the traditional optimization tools used to evaluate the objective function. It has been understood from [4,5,6] that classical, gradient, and conventional optimization techniques have not been successful in getting optimum solutions. To obtain global optimal solutions, researchers have used Metaheuristic Optimization Techniques (MOT) based search for the past three decades. The merits of MOT are that it may escape local optima during optimization due to the stochastic patterns; it has a high level of accuracy in identifying the global optimal solution, robustness, simplicity, reduced computational time, and efficient handling of discrete, complicated, non-linear, and large dimensional optimization problems [6].

1.1 Related Past Works

P_{LS} reduction cost with capacitor investment cost minimization as objective, optimal allocation and sizing of capacitors using Ant Colony Optimization Algorithm (ACOA) has been proposed in [7]. This work adopts a two-phase procedure to solve the objective function. In the first phase, two loss sensitivity indices have been utilized to identify the most decisive nodes for reactive power optimization and optimal capacity has been done by ACOA. In the second phase, both the selection of optimal nodes and capacity determination have been done by ACOA. This work considers both fixed and switched capacitors under three different cases. Minimizing energy loss with capacitor purchase cost as an objective, optimal allocation of capacitors using the Crow Search Algorithm (CSA) has been proposed in [8]. This paper considers all nodes as potential nodes to insert them and enhance the search space. Apart from the objective, this paper also evaluates transformer capacity (MVA) release, line loading capacity, and node voltage improvement before and after reactive power compensation. A combined optimization approach (based on COA, SSA, and loss sensitivity analysis) as an optimization tool, optimal placement, and capacity determination of capacitors in EPDS to minimize power and energy losses have been performed in [9]. Two loss sensitivity factors, VLSF and QLSF (voltage-based and reactive power-based), have been utilized to select the most critical nodes for capacitor placement. SSA / COA optimizes the appropriate sizing for each node after normalization.

P_{LS} and E_{LS} reduction as objectives, optimal location, and appropriate sizing of capacitors in two EPDS have been presented in [10]. In this paper, a two-stage optimization approach has been utilized. To reduce the search space of the optimization tool, normalized LSF and voltage magnitude with fuzzy logic control have been engaged to determine the most potential nodes for reactive power compensation in the first stage of the optimization process. During the second stage, SSA has been engaged to determine the most appropriate capacitor size for each candidate node.

Similar to [10], this paper [11] also focused on P_{LS} and E_{LS} minimization using analytical (using LSF with fuzzy logic controller) and hybrid optimization techniques (hybrid SSA_SCA) in EPDS. LSF has done optimal node selection for capacitors with fuzzy logic controller and the necessary sizing has been done by the respective optimization techniques.

P_{LS} and total voltage deviation minimization as objective, optimal allocation, and sizing of capacitors using the Firefly Algorithm (FA) have been developed in [12]. In this work, the Voltage Stability Index (VSI) has been applied to find the optimal nodes for reactive power compensation and optimal capacitor sizing has been carried out by FA.

Optimal placement and sizing of capacitors using the Cuckoo Search Algorithm (CSA) with weight-based objective function comprises of P_{LS}, Q_{LS}, and VSI has been analyzed in [13]. Similar to the above-discussed papers, this paper also adopts normalized LSF to identify the most appropriate nodes for optimal location and CSA has performed the necessary sizing.

P_{LS} minimization, economic-based penetration of shunt capacitors, and VSI as objective, optimal allocation, and sizing of capacitors in EPDS using the Cuckoo Search Algorithm (CSA) have been reported in [14]. In this work, a penalty factor for voltage violation has been considered. This work investigates

the capacitor allocation starting from single to three optimal nodes.

Many of the authors adopt the Sensitivity Index (SBI) to select appropriate nodes for reactive power compensation [7, 9-13]. Though SBI helps in reducing the search space during optimization, it may not always disclose the appropriate node for RPI or there is no guarantee that the selected node by SBI is the best node for compensation [15]. Also, identifying the most sensitive nodes using SBI will underutilize the MOT.

It is understood from the literature that though modern MOTs attract researchers, some of the MOTs have major problems such as suffering from local optimality, requiring large time for simulation, premature or slow convergence in the refined search stage, partial optimism, scattering problem, weak local search ability, and possible entrapment in local minima, etc. [16,17]. Hence, it is advisable to use a fast, simple, and efficient MOT to solve reactive power compensation problems in complex EPDS to overcome the problems mentioned above, which are obligatory.

1.2 Proposed Work

A new, best, durable, and proficient Meta-Heuristic Optimization Technique (MOT) named Cheetah optimizer (CO) [18] utilizing the concept of hunting strategies of cheetahs has been applied in this work for optimal allocation and capacity determination of RPI. CO has been identified as a powerful MOT in solving many optimization problems to surmount the above-mentioned difficulties. The principal objective of this work is to achieve maximum FS by contemporary optimization of P_{LS} and Q_{LS} reduction cost with capacitor investment cost. This optimization approach (CO) has been tested and validated on three practical EPDS (under four different load variations): a 30-node EDDN-UEN, a 34-node south-west Nigerian Distribution system, and a real 84-node EPDS. The performance of the proposed MOT has been concluded based on the simulation results and comparison studies.

1.3 Purpose and Contribution

With the above-discussed features, the contributions of this work include (i) Suggesting a best and robust MOT called CO to solve the Financial-based objective function (FBOF) (ii) Cost-based assessment of P_{LS} and Q_{LS} reduction with capacitor purchase cost considering four load variations and (iii) For the first time, optimal placement and sizing of capacitors considering four different load variations such as 50%, 75%, 100%, and 125% to solve practical EPDS mentioned above.

The entire paper has been arranged in five sections. Section 2 deals with the problem statement, objective function, and EPDS load flow. Section 3 presents the overview of the solution methodology with the ability to solve RPIs. Section 4 discusses the details of the test system, simulation, and the results obtained with the comparison, and finally, section 5 concludes the work carried out followed by references.

2.0 PROBLEM DEFINITION

This research work intends to achieve maximum FS by allocation and capacity determination of shunt capacitors in three real radial EPDS with the condition to satisfy both network equality and inequality constraints. Before discussing the objective function, it is better to discuss the EPDS Load Flow (EPDSLF) used in this research work.

2.1 Electric Power Distribution System Load Flow (EPDSLF)

To appraise the efficiency of the EPDS under normal operating conditions, a Load Flow (LF) has been performed frequently to identify the requirement of additional power supply necessary to satisfy during the seasonal periods, adequate reactive power support and to ensure the bus voltage profiles within the acceptable limits. The renowned matrix-based PF studies such as Gauss-Seidel, Newton-Raphson, and Fast-Decoupled have proved to be vain in solving EPDS because of the high R/X ratio and radial character [19,20]. In this paper, the quick, robust, capable, and flexible method of EPDSLF developed in 2003[21], which is designed based on the recursive function and a linked-list data structure has been employed to solve the reactive power optimization problem effectively. Total PLS and QLS (summing up all the branches including laterals and sub-laterals) of the entire EPDS may be expressed as given below:

$$P_{LS} = \sum_{b=1}^{TN} P_{Loss(b)} \quad (1)$$

$$Q_{LS} = \sum_{b=1}^{TN} Q_{Loss(b)} \quad (2)$$

Where,

$$p_{loss(b)} = \frac{P_{(b+1)}^2 + Q_{(b+1)}^2}{\left|V_{(b)}^2\right|} \times R_{(b,\ b+1)} \quad \text{and}$$

$$q_{loss(b)} = \frac{P_{(b+1)}^2 + Q_{(b+1)}^2}{\left|V_{(b)}^2\right|} \times X_{(b,\ b+1)}$$

where P_{LS} and Q_{LS} are the sum of real and reactive power losses of all the branches of the EPDS. P_{b+1} and Q_{b+1} represent real and reactive power flow of the $(b+1)^{th}$ branch in kW, kVAR respectively. R_b and X_b are the resistance and inductance of the branch connecting 'b' and 'b+1' in Ω. TN is the total number of branches in the EPDS.

2.2 Problem of Statement - FBOF

Maximize: $$FS = \left[\frac{OF_1 - OF_2}{OF_3 + OF_4}\right] \quad (3)$$

where,

$$OF_1 = K_Q^{PS} \times \left(Q_{(r)}^{D(T)} + Q_{LS(r)}^{AQC}\right)$$

$$OF_2 = \left[\left(\sum_{s=1}^{NN} Q_{C(s,r)} \times K_{Cap}\right) + \left(NN \times K_{IO\&M}\right)\right]$$

$$OF_3 = (K_P^{PS} \times P_{LS(r)}^{AQC})$$

$$OF_4 = (K_Q^{PS} \times Q_{LS(r)}^{AQC})$$

Subject to equality constraints:

$$Q_{PS(r)}^{AQC} - Q_{(r)}^{D(T)} + \sum_{s=1}^{NN} Q_{C(s,r)} - Q_{LS(r)}^{AQC} = 0 \quad (4)$$

Inequality Constraints:

$$\left(\sum_{s=1}^{NN} Q_{C(s,r)} \le \left(Q_{(r)}^{D(T)} + Q_{LS(r)}^{AQC}\right)\right) \quad (5)$$

$$Q_{C(r)}^{\min} \le Q_{C(r)} \le Q_{C(r)}^{\max} \quad (6)$$

$$V_r^{\min} \le V_r \le V_r^{\max} \quad (7)$$

Where K_P^{PS} and K_Q^{PS} refers to cost factor related to real and reactive power from the Primary Source (PS). 'r', AQC, D(T), Q_C, NN, and V indicate the load level, after reactive power compensation, total demand, capacity of the capacitor, total number of compensation nodes and node voltage respectively.

3.0 PROPOSED OPTIMIZATION METHOD (CO)

3.1 Introduction to Meta-Heuristics Technique

The superior advantage of the meta-heuristic optimization technique is it enables the efficient exploration of a large search space by testing a subdivision containing elucidations that could ordinarily be excessively sizeable to be wholly recapitulated or explored. Almost in all such metaheuristics, we employ a fitness function to evaluate the candidate solutions. This is to sample the best solutions so far to focus on exploitation. Further, we use certain aspects of the search strategy to bring randomness and emphasize exploration. This is unique to every search strategy and hence quite difficult to represent using a general formulation. We can use these metaheuristics to solve multi-dimensional real-value functions without relying on their gradient [22,23].

3.2 Overview of the Proposed Meta-heuristic Optimization Technique (CO)

A novel, best, and most robust Meta-heuristic Optimization Technique (MOT) named cheetah Optimizer (CO) inspired by the hunting behavior of cheetahs was developed by Mohammad Amin Akbari in 2022. Cheetahs are known for their incredible speed and agility, making them one of the fastest wild animals. Cheetahs have sharp eyesight, which they use to scan the surroundings for potential prey. They often perch on elevated vantage points like termite mounds, rocks, or tree branches to better view their surroundings (the prey). Once a cheetah spots a potential prey, it starts stalking slowly and cautiously to get closer without being detected. Their spotted coat helps them blend with the grass and vegetation. Cheetahs get as close to their prey as possible before initiating a high-speed chase. They usually try to attack within 50 meters (164 feet) or less of their target. When the distance is right, the cheetah bursts into action, sprinting after its prey. During a chase, a cheetah can reach up to 60 to 70 miles per hour (97 to 113 kilometers per hour) for short distances, covering around 500 meters (1,640 feet). These sprints are intense but brief, lasting typically less than a minute. Once the cheetah catches up its prey, it uses its sharp, retractable claws to trip the prey by swiping at its hind legs. This action disrupts the prey's balance and causes it to stumble or fall. Once the prey is down, the cheetah quickly moves in to deliver a precise and powerful bite on its throat, suffocating the prey and ensuring a quick kill. After successfully bringing down its prey, the cheetah may drag it to a more secluded spot to avoid scavengers.

The Cheetah Optimizer (CO) has been utilized in this study because of its demonstrated effectiveness in resolving challenging optimization issues, especially when a balance between exploration and exploitation is needed. It is a good fit for the reduction in real and reactive power loss in radial power distribution systems because of its quick convergence, ease of use, and capacity to manage non-linear and multi-modal problems. The work's success compared to traditional methods is demonstrated by the notable reductions in power losses and enhanced financial savings achieved by applying CO.

3.3 Mathematical Modeling

The hunting behavior of cheetahs serves as a clever inspiration for developing the Cheetah Optimizer (CO) algorithm, effectively channeling their natural strategies into a computational framework. The tactics are structured into three phases: search, sit-and-wait, and attack.

3.3.1 Search Strategy

Cheetahs employ a dual approach in their prey search. They either meticulously scan their surroundings from a seated or standing position or actively engage in patrolling the search area. The decision to employ the scanning mode is optimal when the prey is densely clustered and grazing on open plains. Conversely, opting for the active mode,

which demands greater energy expenditure, is more advantageous when the prey is scattered and actively moving. The choice of search mode is contingent upon the prevailing circumstances for the cheetah, the state of the prey, and the extent of the area under scrutiny. Within the mathematical framework, the present position of cheetah "i" (where i ranges from 1 to n) within arrangement "j" (ranging from 1 to D) holds significance. Here, "n" denotes the count of cheetahs, and "D" signifies the dimension of the optimization challenge. Each cheetah navigates distinct circumstances stemming from its prior interactions with prey. These prey, embodying decision variables, encapsulate optimal solutions. As such, the states of the cheetahs collectively compose a population, mirroring the dynamics of this ecosystem.

$$X_{i,j}^{t+1} = X_{i,j}^{t} + \hat{r}_{i,j}^{-1}.\ \alpha_{i,j}^{t} \tag{8}$$

Where $X_{i,j}^{t+1}$ and $X_{i,j}^{t}$ represents current and past positions of the cheetah 'i' in an arrangement j respectively. Here $X_{i,j}^{t+1}$ indicates the new arrangement of cheetah 'i' at hunting time 't.' $\hat{r}_{i,j}^{-1}$ signifies a randomized variable, which takes on values drawn from a standard normal distribution, characterized by its mean of 0 and standard deviation of 1. $\alpha_{i,j}^{t}$ represents the step length, typically a positive value which is expressed (leader) as,

$$\alpha_{i,j}^{t} = 0.001 \times \left(\frac{t}{T}\right) \times \left(UB_j - LB_j\right) \tag{9}$$

where UBj and LBj are the upper and lower limits of the variable 'j'. 'T' represents the maximum hunting time and 't' specifies the current hunting period. For other members of a group of cheetahs, the random step length is expressed based on the distance of the cheetah 'i' and arbitrarily selected cheetah 'k' in a group as follows [18]:

$$\alpha_{i,j}^{t} = 0.001 \times \left(\frac{t}{T}\right) \times \left(X_{i,j} - X_{k,j}\right) \tag{10}$$

In response to encounters with other hunters, cheetahs swiftly change direction and evade. This behavior coupled with near/far destination modes is emulated using the random variable for each cheetah across hunting periods. Adaptations in "α_t" might involve cheetah proximity or leadership. The leader's position is updated by setting it to 0.001 times "t/T" multiplied by the maximal step size based on variable limits. For others, depends on the distance to a random cheetah. The leader adjusts to the prey's position by modifying some variables. Over time, leader and prey closeness evolves unless hunting ends, yielding updated leadership. Cheetah step size randomness in CO effectively solves optimizations using randomized parameters and steps.

3.3.2 Sit-and-Wait Strategy

In the search phase, the prey might enter a cheetah's field of view. In such instances, the slightest movement by the cheetah could alert the prey, prompting its escape. To circumvent this, the cheetah might lay low (on the ground or within foliage) to approach the prey discreetly. Consequently, the cheetah remains stationary in this mode, awaiting the prey's proximity. This behavior can be depicted as follows:

$$X_{i,j}^{t+1} = X_{i,j}^{t} \tag{11}$$

This approach necessitates the CO algorithm to refrain from altering all cheetahs simultaneously within each group. This strategic decision enhances hunting success (achieving improved solutions) and effectively helps prevent premature convergence.

3.3.3 Attack Strategy

Cheetahs employ speed and flexibility to attack prey. Upon initiating an attack, cheetahs rush towards the prey, adapting direction based on their movement. They aim to intercept prey by positioning themselves strategically. Cheetahs adjust positions based on fleeing prey, leader, or neighbors in group hunting. Mathematically, attack tactics are represented as:

$$X_{i,j}^{t+1} = X_{B,j}^{t} + \breve{r}_{i,j}.\beta_{i,j}^{t} \tag{12}$$

Here, $X_{B,j}^{t}$ mirrors the prey's best position, $\breve{r}_{i,j}$ and $\beta_{i,j}^{t}$ are turning and interaction factors for cheetah "i" in arrangement "j," and $\breve{r}_{i,j}$ are random variables reflecting sharp turns.

$$\breve{r}_{i,j} = \left|r_{i,j}\right|^{\exp(r_{i,j}/2)} \sin(2\pi r_{i,j}) \tag{13}$$

$$\beta_{i,j}^{t} = X_{k,j}^{t} - X_{i,j}^{t} \tag{14}$$

3.3.4 Leaving-prey-and-returning-home Phase

After an unsuccessful attack, cheetahs retreat to their den to replenish their energy before setting out on a fresh hunting expedition. During this time, the cheetah's location is adjusted to match the current position of their prey.

$$X_{ij}^{t} = X_{pj}^{t} \tag{15}$$

The leader's position is reset to the location of the best solution. In addition to this, the hunting time "t" and the positions of the remaining cheetahs are also reset. In CO, the optimization process prioritizes replacing the worst objective solution values with the

best ones discovered. When multiple solutions share the same objective values, random solutions are introduced to replace them. This approach combines selecting top solutions and adding randomness to improve the overall optimization results.

3.4 Implementation of CO for RPI Problem

The proposed CO has been implemented to find the optimal allocation and capacity determination of capacitors in three real EPDS that minimize both P_{LS} and Q_{LS} with enrichment in bus voltage. The CO has been carried out which depends on the following steps:

Step 1: Initialize the variable boundary limits such as the optimal location for capacitor allocation and its sizing, and select the max. number of iterations and population. Generate the initial solution vectors of a size considering all the constraints (4) - (7).

Step 2: Calculate the network parameters such as P_{LS}, Q_{LS} and voltages of all the nodes using the EPDSLF discussed in [21] for each solution vector (SV) generated.

Step 3: Compute the fitness of each cheetah and elect the leader.

Step 4: Based on variables r1, r2, r3, r4, and H, select a suitable strategy and compute the cheetah's new position.

Step 5: Amend the Cheetah based on the upper and lower boundary conditions. Compute the best value for the given fitness function (3)

Step 6: If fitness is not achieved, implement leaving the prey and go back home strategy.

Step 7: The iteration process stops after the successful completion of the final iteration. Final value of the objective function (FS in $) with the capacitor variable values will be displayed. Otherwise, steps 2 to 7 will be repeated till the minimum value of the objective function is obtained. Art. 3.4 displays the pseudo-code for the proposed reactive power optimization problem using CO.

3.5 Pseudo Code for RPI Problem – CO

Define D, n, $MaxIt$
Generate the initial population of cheetahs Xi (1, 2, …n) and evaluate the fitness of each cheetah
Initialize the population's home, leader, and prey solutions $it \leftarrow 1$
While $it \leq MaxIt$ do
Select $m\ (2 \leq m \leq n)$ members of cheetahs randomly
For each member I ϵ m do
Define the neighbor agent of the member i
For each arbitrary arrangement j ϵ {1,2,3… D} do
Calculate $\hat{r}, \tilde{r}, \alpha, \beta,$ and H
Apply the strategy selection mechanism to generate a new arrangement according to (8), (11) or (12)
End
Update the solutions of member i and the leader
End
Apply leave the prey and go back home strategy
$it \leftarrow it + 1$
Update the prey (global best) solution
End

4.0 CASE STUDY DETAILS, SIMULATION RESULTS AND DISCUSSIONS

To substantiate the effectiveness of the developed MOT (CO) in optimizing the financial-based objective function (discussed in section 2), three practical EPDS have been taken, and simulations have been carried out for four different load variations.

To reflect a wide variety of operating situations commonly found in radial power distribution systems, load variations of 50%, 75%, 100%, and 125% were selected. This range ensures that the suggested capacitor allocation approach is reliable and efficient in a variety of real-world scenarios by considering low-demand scenarios (50%), moderate demand (75%), peak demand (100%), and overloaded conditions (125%). These variances aid in assessing the system's performance in both typical and extreme scenarios, offering valuable information about its dependability and practicality. The details of the three EPDS are discussed in Art. 4.1

4.1 Case Study Details

The first practical EPDS is a real 2-feeder, 30-node EDDN-UEN. The single-line diagram of the 30-bus EDDN-UEN is shown in Figure 1. It has 30 nodes and 29 branches with a looping branch. This network is an 11KV network with a total connected load of 27383.367 kVA at 0.84893 Power Factor [7], considering 100% load.

The second illustration taken for evaluation is Ayepe 11 KV, 34-node feeder of the Ibadan Electricity Distribution Company (IBEDC), Ibadan, Nigeria, supplying from 33/11 KV, 15 MVA transformer located at Osogbo, South-West Nigeria.

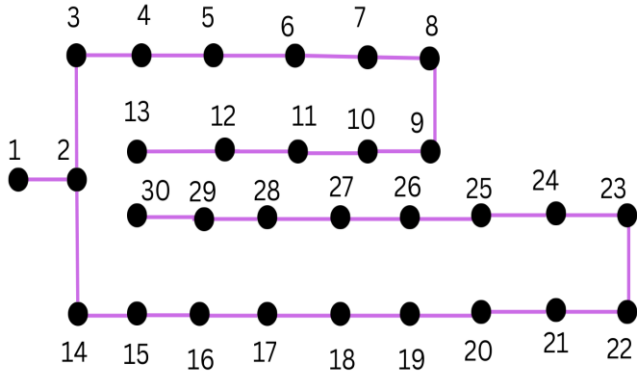

Figure 1 Single line diagram of 30 nodes EDDN-UEN EPDS

The EPDS has 34 nodes and 33 branches without any looping branches. The total connected load of the EPDS is 5351.161 kVA at 0.911885 PF [12] considering 100% load. The One-line diagram of the Ayepe 11 KV feeder network is shown in Figure 2.

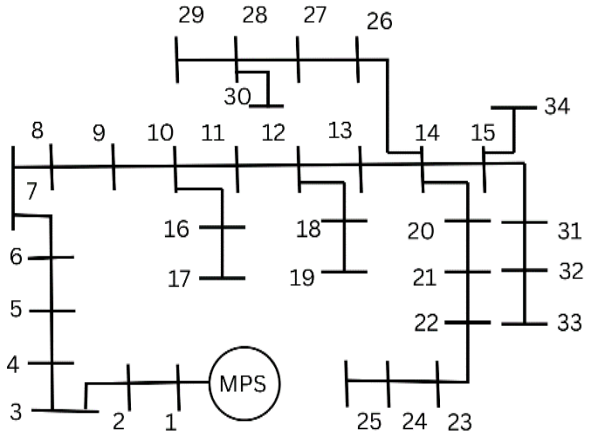

Figure 2 Single line diagram of 34 nodes Nigerian Ayepe feeder

The final system considered here is a real EPDS of TPC [24]. The operating voltage of the EPDS is 11.4 KV. It has 11 feeders, 84 nodes, and 83 branches with 13 looping branches. The connected load of the EPDS is 36351.6757 kVA at 0.794516 PF. The single-line diagram of 84-bus EPDS is shown in Figure 3 [25].

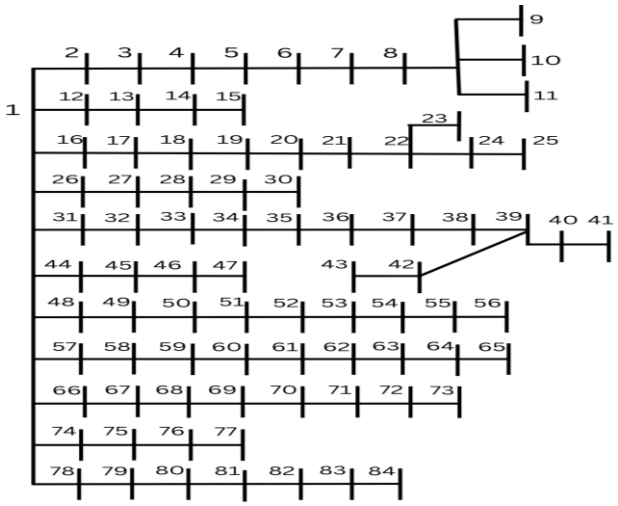

Figure 3 Single-line diagram of a real 84-node TPS EPDS

The line and bus data have been taken from [24]. The details on total apparent power loss, minimum node voltage, and economic loss considering all the four load variations under Before Optimization (BO) of the EPDS for all the above-discussed EPDSs are tabulated in Table 1.

Table 1 Parameter details of EPDS under 4 different load variations – BO

Load variation	Load demand (P +j Q) (kVA) / Power Factor	P_{LS} + j Q_{LS} (kVA)	V_{min} (p.u.)	Cost of (P_{LS}+ Q_{LS})
	30 node EDDN-UEN system			
50%	(11414.326 +j 7155.6254) / 0.84727	(193.326+j 74.5254)	0.9751	$9293.95
75%	(17274.807 +j 10792.981) / 0.84808	(443.807 +j 170.981)	0.9629	$21334.11
100%	(23246.6112 +j 14472.1753) / 0.84893	(805.6112 + j310.1753)	0.9501	$38723.5264
125%	(29338.4 +j 18197.9484) / 0.8498	(1286.4 +j 494.9484)	0.9222	$61828.91
	Nigerian AYEPE 34 node EPDS			
50%	(2215.8132 +j 1055.1914) / 0.902854	(157.3132 +j 30.1914)	0.9229	$7130.26
75%	(3474.3847 +j 1611.693) / 0.90715	(386.5847 +j 74.193)	0.8789	$17522.05
100%	(4879.6417 +j 2196.3652) / 0.911885	(762.6417 +j 146.3652)	0.8295	$34566.92
125%	(6501.3 +j 2822.5666) / 0.91728	(1355.1 + j 260.0666)	0.7721	$61420.206
	Real 84-node EPDS			
50%	(14302.2119 +j 10678.5309) / 0.80129	(127.2119 +j 328.5309)	0.9657	$10084.366
75%	(21555.5018 +j 16280.516) / 0.797972	(292.5018 +j 755.516)	0.9475	$23188.9
100%	(28881.9945 +j 22074.3) / 0.79451618	(531.9945 +j 1374.3)	0.9285	$42178.03
125%	(36289.487 +j 28075) / 0.7909356	(851.487 +j 2200)	0.9085	$67513.346

Node number 1 has been taken as a slack bus / sub-station bus for all the practical EPDS. Other than node no. 1, all other nodes are considered as load nodes. For the slack bus, the node voltage has been fixed as 1 p.u. Reactive power compensation has been done on any potential nodes from node number 2 to the end node of the EPDS. In this work, reactive power compensation has been done on 4 nodes for a 30-node EDDN-UEN, 3 nodes for a 34-node Nigerian Ayepe feeder, and 5 nodes for an 84-node practical EPDS.

The proposed algorithm with EPDSPF has been developed and carried out in MATLAB software and runs on an i5 Intel processor with 8 GB RAM. The Solution Vector (SV) size and number of iterations have been selected as 800 and 100, respectively. For each node of reactive power compensation, two variables are assigned (optimal node and optimal sizing).

The parameter setting for CO has been considered as given in [18]. The real power cost (K_P^{PES}) has been considered as $42.6 / kW [26]. From

[27], it is understood that the cost of the reactive power (K_Q^{PES}) is considered to be one–third of the real power cost. The purchase cost of the capacitor has been taken as \$0.5 / kVAR [28]. Capacitor-associated costs such as installation, operation, and maintenance costs (I, O & M) have been taken as \$43.6 / node [29]. Base KV for the first two EPDSs are taken as 11 KV and for the third EPDS, it is 11.4 KV. For all the EPDS, the base MVA has been considered as 100 MVA. To investigate the supremacy of the CO in suppressing real and reactive power loss and capacitor investment cost, all the three real EPDSs underwent simulations to identify the effect of cost savings under four different load variations.

4.2 Results and Discussions – 30-Node EPDS-Nigerian Ayepe Feeder

First, the suggested MOT has been applied for 30-node EDDN-UEN for 50% to 125% load variations in steps of 25%. The parameter details on all the four load variations under BO are shown in Table 1. The results achieved by CO are tabulated in Table 2. It is evident from Table 2 that, the real and reactive power loss reductions between 25.8% and 27.64% are observed with the reactive power penetrations between 60% and 69.3%. The minimum node voltage differences between BO and AO under all four load variations are 0.005 p.u., 0.0085 p.u., 0.0134 p.u., and 0.0142 p.u. respectively. There is a gradual increase in FS noticed for all the load variations. From Table 3, it is obvious that a minimum and a maximum P_{LS} reduction difference of 0.013% to 15.103% are observed. However, AO, the V_{min} is less than other optimization methods. From Table 3, it is also apparent that the P_{LS} reduction increases with increased reactive power penetration. The V_{min} achieved by the proposed method is less compared to other methods. Figure 4 shows the node voltage of 30-node EDDN-UEN under BO and AO for all four load variations.

Table 2 Performance of CO – All the four load variations – 30-node EDDN-UEN

Parameters	50% Load	75% Load	100% Load	125% Load
P_{LS} – AO / BO (kW)	142.7 / 193.326	322.8955 / 443.807	583.96 / 805.6112	931.311 / 1286.4
Q_{LS} – AO / BO (kVAR)	55.305 / 74.5254	124.9109 / 170.981	225.7223 / 310.1753	360.0754 / 494.9484
% P_{LS} reduction	**26.186**	**27.244**	**27.523**	**27.64**
% Q_{LS} reduction	**25.7904**	**26.9445**	**27.2275**	**27.25**
V_{min} (p.u.) & (Bus No.) – AO / V_{min} (p.u.) & (Bus No.) – BO	0.9751 (29,30) / 0.9701 (29,30)	0.963 (29,30) / 0.9545 (29,30)	0.953 (29,30) 0.9386 (29,30)	0.9364 (29,30) 0.9222 (29,30)
Capacitor rating (kVAR) & (Node)	1249 (7) 988 (16) 1497 (20) 560 (25)	2245 (7) 2022 (16) 2358 (20) 854 (25)	3068 (7) 2644 (16) 3057 (20) 1226 (25)	3516 (7) 3275 (16) 3648 (20) 1430 (25)
% Capacitor penetration	60.0085	69.297	69.0623	65.2222
ΔP_{LS} cost (\$) – (A)	2156.668	5150.83	9442.34	15126.79
ΔQ_{LS} cost (\$) – (B)	272.93	654.1954	1199.233	1915.1966
Capacitor investment cost (\$) (C)	2321.4	3913.9	5171.9	6108.9
F S (\$) [(A+B) – (C)]	**108.198**	**1891.1254**	**5469.673**	**10933.1**

Table 3 Comparison of 30 node EDDN-UEN – 100% load variation

Parameters		P_{LS} (kW) (AO / BO)	% P_{LS} reduction	V_{min} (p.u.) & (Bus No.)	Capacitor rating (kVAR) & (Node)	% Capacitor Penetration
ACO (2016) [7]	**Case 1**	648.148 / 805.73	19.56	0.9539 (29,30)	1147(18) 1180 (20) 1167 (21) 1180 (25)	33
	Case 2	646.383 / 805.73	19.78	0.9529 (29,30)	1200 (9) 1200 (18) 1200 (21) 1200 (25)	33.8935
CSA (2017) [8]		705.673 / 805.7368	12.42	---------	600 (21) 600 (22) 600 (24) 750 (26	18
COA (2018) &	**P_{LS} reduction**	622.0176 / 805.73	22.8	0.9568 (30)	2100 (18) 2100 (19)	51.9

Parameters		P_{LS} (kW) (AO / BO)	% P_{LS} reduction	V_{min} (p.u.) & (Bus No.)	Capacitor rating (kVAR) & (Node)	% Capacitor Penetration
SSA [9]					2100 (21) 1050 (25	
	E_{LS} Cost minimization	629.41314 / 805.73	14.16	0.9551 (30)	2100 (18) 1650 (19) 1350 (22) 900 (25)	42.367
	P_{LS} reduction	646.02 / 805.737	19.822	---------	1200 (18) 1200 (20) 1200 (21) 1200 (25)	33.8935
SSA (2019) [10]	**E_{LS} Cost minimization**	692.56 / 805.737	14.0464	---------	725 (20) 500 (21) 800 (23) 725 (26)	19.4182
SSA_SCA (2020) [11]	**P_{LS} reduction**	584.05 / 805.735	27.51	0.956 (30)	2500 (7) 2500 (15) 2500 (18) 2500 (23)	70.6115
	E_{LS} cost reduction	595.50 / 805.73	26.09	0.9554 (30)	1960 (7) 2189 (17) 2992 (20) 1110 (25)	58.26155
CO		583.96 / 805.6112	**27.523**	0.953 (29,30)	3068 (7) 2644 (16) 3057 (20) 1226 (25)	69.0623

4.3 Results and Discussions – 34-node Nigerian Ayepe Feeder

The next real EPDS taken for evaluation is a 34-node Nigerian Ayepe feeder. The parameter details of this EPDS have already been discussed in Art. 4.1. This real EPDS also simulated for four different load variations and the results are recorded in Table 4. From Table 4, it is understood that the reduction of P_{LS} and Q_{LS} under all the load variations is almost the same. The difference between the P_{LS} and Q_{LS} reduction across all the load variations is found to be 3.646%. Around a 1% difference in both the loss reductions between each load variation is noticed. Similarly, the increase in the penetration of reactive power considering all four load variations is found to be minuscule. The V_{min} difference between BO and AO under four different load variations are 0.0071 p.u., 0.012 p.u., 0.0185 p.u. and 0.0272 p.u. respectively. The FS increases with load variations. Table 5 shows the comparison of the results obtained by CO with the other methods available in the literature. The proposed method achieves a better performance than Firefly [12], a two-stage method [13], and CSA [14]. However, there is no difference in V_{min} between CO and [13,14]. Figure 5 shows the node voltage profile for the 34-node Nigerian Ayepe feeder under BO and AO for all four load variations.

Table 4 Performance of CO All the four load variations: 43 node Nigerian Ayepe feeder

Parameters	50% Load	75% Load	100% Load	125% Load
P_{LS} – AO / BO (kW)	124.3561 / 157.3132	302.4241 / 386.5847	587.801 / 762.6417	1021.8 / 1355.1
Q_{LS} – AO / BO (kVAR)	23.8663 / 30.1914	58.0409 / 74.1929	112.8115 /146.3652	196.1035 / 260.0666
% P_{LS} reduction	20.95	21.7703	22.9246	24.596
% Q_{LS} reduction	20.95	21.7703	22.9246	24.595
V_{min} (p.u.) & (Bus No.)–AO / V_{min} (p.u.) & (Bus No.) – BO	0.93 (25) / 0.9229 (25)	0.8909 (25) / 0.8789 (25)	0.8481 (25) / 0.8295 (25)	0.7993 (25) / 0.7721 (25)
Capacitor rating (kVAR) & (Node)	215 (9) 498 (14) 191 (31)	291 (9) 818 (14) 252 (31)	462 (9) 1087 (14) 289 (31)	507 (9) 1296 (14) 512 (31)
% Capacitor penetration	88.195	88.52	89.6585	90.3415
ΔP_{LS} cost ($) – (A)	1403.9725	3585.2416	7447.8773	14198.58
ΔQ_{LS} cost ($) – (B)	89.8164	229.358	476.4625	908.276
Capacitor inv. cost ($)(C)	582.8	811.3	1049.8	1288.3
FS ($) [(A+B) – (C)]	**910.9889**	**3003.3**	**6874.54**	**13818.556**

Table 5 Comparison of 43 node Nigerian Ayepe feeder EPDS – 100% load variation

Parameters	Firefly [12]	Two-stage method [13]	CSA [14]	C O
P_{LS} (kW) – AO	597.7486	588.09	588.09	587.801
P_{LS} (kW) – BO	762.6419	762.64	762.64	762.6417
Q_{LS} (kVAR) – AO	-----	112.87	112.87	112.8115
Q_{LS} (kVAR) - BO	-----	146.37	146.37	146.3652
% P_{LS} reduction	21.62	22.8876	22.8876	22.9246
% Q_{LS} reduction	-----	22.8872	22.8872	22.9246
V_{min} (p.u.)& (Bus No.)	0.8456 (25)	0.8481 (25)	0.8481 (25)	0.8481 (25)
Capacitor rating (kVAR) & (Node)	400 (23) 600 (24) 500 (32)	800 (10) 550 (21) 500 (31)	800 (10) 550 (21) 500 (34)	462 (9) 1087 (14) 289 (31)
% Capacitor penetration	73.171	90.244	90.244	89.6585

4.4 Results and Discussions – Real TPC EPDS [19]

The final discussion is based on the real EPDS of TPC. For the sake of simplicity, tie-switches are not shown in the diagram. The results obtained by CO for all the load variations are tabulated in Table 6. It is observed from Table 6 that, similar to the 34-node Nigerian Ayepe feeder this TPC EPDS also yields almost equal reductions in P_{LS} and Q_{LS}. The capacitor's penetrations are found to be between 36% and 39%. The V_{min} differences between BO and AO under four different load variations are 0.0179 p.u., 0.0273 p.u., 0.0381 p.u., and 0.0493 p.u. respectively. It is evidenced that the FS is found to be increasing. Figure 6 shows the node voltage profile for 84 node EPDS of TPC under four different load variations.

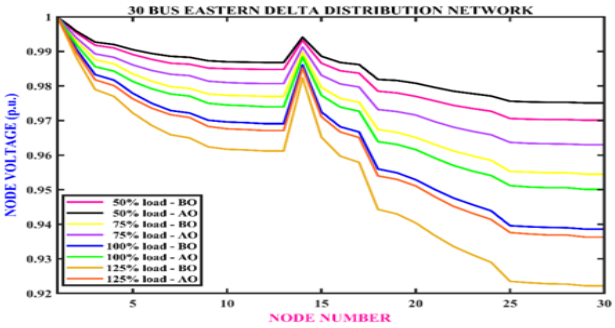

Figure 4 Node Voltage Profile– 30 node EDDN– All load variations

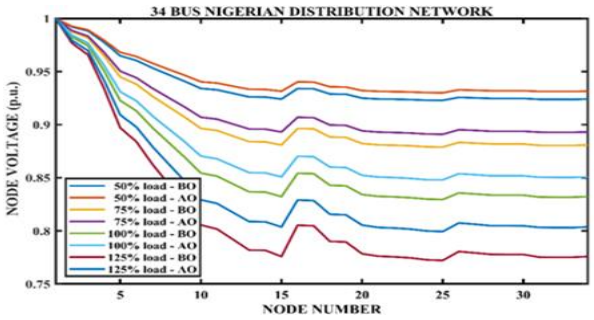

Figure 5 Node Voltage Profile- 34 node Ayepe feeder

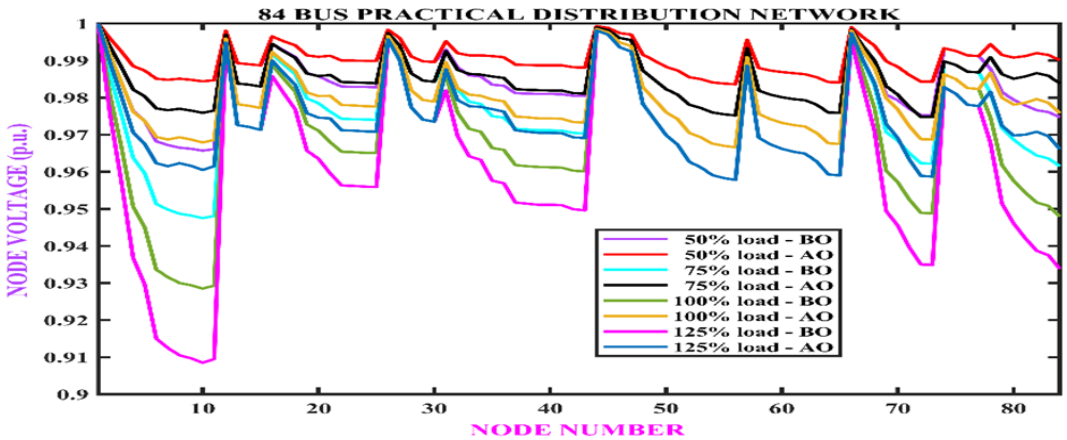

Figure 6 Node Voltage Profile – 84 node – TPC EPDS – All load variations

Table 6 Performance of CO – All the four load variations – Real 84 node EPDS of TPC

Parameters	50% Load	75% Load	100% Load	125% Load
P_{LS} – AO / BO (kW)	98.7491 / 127.2119	226.4045 / 292.5018	407.8507 / 531.9945	646.2137 / 851.487
Q_{LS} – AO / BO (kVAR)	253.9037/ 328.5309	582.5168 / 755.5161	1049.3 / 1374.3	1666.6 / 2200
% P_{LS} reduction	22.3743	22.59723	23.3355	24.10763
% Q_{LS} reduction	22.71543	22.8982	23.6484	24.24545
V_{min} (p.u.) & (Bus No.) – AO / V_{min} (p.u.) & (Bus No.) – BO	0.9836(56)/ 0.9657(10)	0.9748 (72,73) / 0.9475 (10)	0.9666 (56) / 0.9285 (10)	0.9578 (56) / 0.9085 (10)
Capacitor rating (kVAR) & (Node)	965 (8) 661 (21) 736 (35) 682 (69) 982 (82)	1437 (8) 922 (21) 1011 (35) 924 (69) 1403 (82)	1948 (8) 1158 (21) 1223 (35) 1443 (69) 1726 (82)	2513 (8) 1354 (21) 1787 (35) 1698 (69) 1953 (82)
% Capacitor penetration	38.8985	36.6956	36.2222	35.9613
ΔP_{LS} cost ($) – (A)	1212.5153	2815.745	5288.5256	8744.6426
ΔQ_{LS} cost ($) – (B)	1059.7062	2456.59	4615	7574.28
Capacitor investment cost ($) – (C)	2231	3066.5	3967	4870.5
F S ($) [(A+B)–(C)]	**41.2215**	**2205.835**	**5936.5256**	**11448.423**

5.0 CONCLUSIONS

This work adopts a powerful MOT named Cheetah Optimizer (CO) to know the optimal variations in penetration of capacitors to achieve maximum real and reactive power loss minimization with a reduction in capacitor investment cost, thereby more FSs. The merits of adopting CO for this problem have already been discussed. The developed methodology has been validated using three real EPDS: a 30-node EDDN-UEN, a 34-node Nigerian Ayepe feeder, and an 84-node EPDS of TPC.

From the above discussions, it is clear that no sensitivity factor-based index has been adopted in this paper to select optimal nodes for reactive power compensation. CO has to identify the most potential nodes and the appropriate reactive power capacity of the capacitor. Considering the 30-node EDDN-UEN, around 27% of PLS and QLS reductions have been noticed, considering all four load variations with an FS between $108 and $10933 is evidenced. Regarding the 34-node Nigerian Ayepe feeder, the reduction in real and reactive power losses are found to be between 21% and 24.5%, with a reactive power penetration of around 90%. Thus, the FS increases steadily from $910 to $13818 for 50% to 125% load variations. Taking into consideration the 84-node EPDS of TPC, the reductions in both the losses are found to be between 22% and 24%, with the reactive power penetration of around 38% is evidenced. The FS under all four load variations are found to be between $41 and $11448.

Considering the 30-node EDDN-UEN and 34-node Nigerian Ayepe feeder, the performances have been compared to the recent methods presented in the literature. The difference in PLS and QLS reduction achieved by CO are found to be better and significant. From the simulation results and the above discussions, it is clear that CO yields better performance than other methods in terms of PLS and QLS reduction. Hence, CO has been recommended to be another strong and efficient method for solving reactive power optimization.

Acknowledgment

Our sincere gratitude to Mr. K. Karthikeyan, Senior Maintenance Engineer, Tagore Medical College & Hospital, Rathinamangalam, CHENNAI, INDIA, for his endless support during my research work, without whom I would not have been in my present position.

Conflicts of Interest

The authors declare that there is no conflict of interest regarding the publication of this paper.

References

[1] S. Haffner, L. F. A. Pereira, L. A. Pereira, and L. S. Barreto, 2008. Multistage Model for Distribution Expansion Planning with Distributed Generation—Part I: Problem Formulation, *IEEE Trans. Power Deliv*. 23(2): 915–923 Doi: 10.1109/TPWRD.2008.917916.

[2] Vasant Surdeo. 2018. Power Sector Policies in India: History and Evolution. *Jindal Journal of Public Policy*. 3: 115–128.

[3] Srinivasan, G., Senthil Kumar, R., & Muthukaruppasamy, S. 2022. Evaluation of Additional Power Loss Reduction in DG Integrated Optimal Distribution Network. *Control Engineering and Applied Informatics*. 24: 68–76.

[4] Gampa, S. R., & Das, D. 2016. Optimum Placement of Shunt Capacitors in a Radial Distribution System for Substation Power Factor Improvement using Fuzzy GA Method. *International Journal of Electrical Power & Energy Systems*. 77: 314–326.

[5] Sultana, S., & Roy, P. K. 2014. Optimal Capacitor Placement in Radial Distribution Systems Using Teaching Learning-Based Optimization. *International Journal of Electrical Power & Energy Systems*. 54: 387–398.

[6] Sultana, S., & Roy, P. K. 2016. Oppositional Krill Herd Algorithm for Optimal Location of Capacitor with Reconfiguration in Radial Distribution System. *International Journal of Electrical Power & Energy Systems.* 74: 78–90.
[7] Adel Ali Abou El-Ela, Ragab A. El-Sehiemy, Abdel-Mohsen Kinawy, & Mohamed Taha Mouwafi. 2016. Optimal Capacitor Placement in Distribution Systems for Power Loss Reduction and Voltage Profile Improvement. *IET Gener. Transm. Distrib.* 10: 1209–1221.
[8] Abdullah M. Shaheen, & Ragab A. El-Sehiemy. 2017. Optimal Allocation of Capacitor Devices on MV Distribution Networks Using Crow Search Algorithm. *24th International Conf. & Exhibition on Electricity Distribution* (CIRED), 12-15 June 2017. 2453–2457.
[9] Abdel-Raheem Youssef, Salah Kamel, Mohamed Ebeed, & Juan Yu. 2018. Optimal Capacitor Allocation in Radial Distribution Networks Using a Combined Optimization Approach. *Electric Power Components and Systems*. 1–19.
[10] Ali Selim, Saleh Kamel, & Francisco Jurado. 2019. Power Losses and Energy Cost Minimization Using Shunt Capacitors Installation in Distribution Systems. *The 10th International Renewable Energy Congress* (IREC 2019).
[11] Ali Selim, Saleh Kamel, & Francisco Jurado. 2020. Capacitors Allocation in Distribution Systems Using a Hybrid Formulation Based on Analytical and Two Metaheuristic Optimization Techniques. *Computers and Electrical Engineering.* 85: 106675.
[12] Olabode E. O., Ajewole T. O., Okakwu I. K., & Ade-Ikuesan O. O. 2019. Optimal Sitting and Sizing of Shunt Capacitor for Real Power Loss Reduction on Radial Distribution System Using Firefly Algorithm: A Case Study of Nigerian system. *Energy Sources, Part A: Recovery, Utilization, and Environmental Effects*. 5(5): 1–13.
[13] Salimon, S. A,, Baruwa, A. A., Amuda, S. O. & Adeleke, H. A. 2020. Optimal Placement and Sizing of Capacitors in Radial Distribution Systems: A Two-Stage Method. *Journal of Engineering Research and Reports.* 19: 31–43.
[14] Salimon, S. A., Suuti, K. A., Adeleke, H. A., Ojo, K. E., & Aderinko, H. A. 2020. Impact of Optimal Placement and Sizing of Capacitors on Radial Distribution Network using Cuckoo Search Algorithm. *IOSR Journal of Electrical and Electronics Engineering* (IOSR-JEEE). 15(1, Series I): 39–49.
[15] Haldar, V., & Chakraborty, N. 2015. Power Loss Minimization by Optimal Capacitor Placement in Radial Distribution System Using Modified Cultural Algorithm. *International Transactions on Electrical Energy Systems*. 25: 54–71.
[16] Sneha Sultana & Provas Kumar Roy. 2014. Multi-objective Quasi-Oppositional Teaching Learning Based Optimization for Optimal Location of Distributed Generator in Radial Distribution Systems. *Electrical Power and Energy System*. 63: 534–545.
[17] Prakash, D. & Lakshminarayana, C. 2017. Optimal Siting of Capacitors in Radial Distribution Network Using Whale Optimization Algorithm. *Alexandria Engineering Journal,* 56: 499–509.
[18] Mohammad Amin Akbari, Mohsen Zare, Rasoul Azizipanah-abarghooee, Seyedali Mirjalili & Mohamed Deriche. 2022. The Cheetah Optimizer: A Nature-Inspired Metaheuristic Algorithm for Large-Scale Optimization Problems. *Scientific Reports*. 12: 10953.
[19] Ramana, T., Ganesh, V., Siranagaraju, S. 2003. Simple and Fast Load Flow Solution for Electrical Power Systems. *International Journal of Electrical Engineering and Informatics.* 5: 245–253.
[20] Kumar, V., Swapnil, S., Ranjan, R., Singu, V. R. 2017. Improved Algorithm for Load Flow Analysis of Radial Distribution System. *Indian Journal of Science and Technology*. 10: 1–7.
[21] Venkatesh, B., Ranjan, R. 2003. Data Structure for Radial Distribution Load Flow Analysis. *IEE Proceedings on Generation Transmission and Distribution*. 150: 101–106. https://doi.org/10.1049/ip-gtd:20030013.
[22] Vinita Tomar, Mamta Bansal and Pooja Singh. 2023. Metaheuristic Algorithms for Optimization: A Brief Review. *Eng. Proc.* 59(1): 238. https://doi.org/10.3390/engproc2023059238.
[23] Kanchan Rajwar, Kusum Deep and Swagatam Das. 2023. An Exhaustive Review of the Metaheuristic Algorithms for Search and Optimization: Taxonomy, Applications, and Open Challenges. *Artificial Intelligence Review*. 56: 13187–13257. https://doi.org/10.1007/s10462-023-10470-y.
[24] Wang, C. & Zhong, H. 2008. Optimization of Network Configuration in Large Distribution System Using Plant Growth Simulation Algorithm. *IEEE Trans. Power Syst.* 23(1): 119–126.
[25] Marco Antonio Leon Ibarra, Jose Leonardo Guardado, Francisco Rivas-Davalos, Jacinto Torres Jimenez & Jose Luis Naredo. 2016. An Elitist Local Search Based Multi-Objective Algorithm for Power Distribution System Reconfiguration. *Electric Power Components and Systems.* 44(16): 1839–1853.
[26] Srinivasan, G., Amaresh, K. & Kumar Reddy Cheepati. 2022. Economic based Evaluation of DGs in Capacitor Allocated Optimal Distribution Network. *Bulletin of the Polish Academy of Sciences: Technical Sciences,* 70(1): e139053.
[27] Hossein Karimi & Reza Dashti. 2016. Comprehensive Framework for Capacitor Placement in Distribution Networks from the Perspective of Distribution System Management in a Restructured Environment. *Electrical Power and Energy Systems.* 82: 11–18.
[28] Chu-Sheng Lee, Helon Vicente Hultmann Ayala, & Leandro dos Santos Coelho. 2015. Capacitor Placement of Distribution Systems Using Particle Swarm Optimization Approaches. Electr. *Power Energy Syst.* 64: 839–851.
[29] Ignacio Pérez Abril. 2020. Capacitor Placement by Variables' Inclusion and Interchange Improved Algorithm. *International Transactions on Electrical Energy Systems.* 30(6): e12377.